

Velocity correlations of vortices and rarefaction pulses in compressible planar quantum fluids

Ashton S. Bradley * and Nils A. Krause 

*Dodd-Walls Centre for Photonic and Quantum Technologies, Dunedin 9054, New Zealand and
Department of Physics, University of Otago, Dunedin 9016, New Zealand*

(Dated: February 14, 2025)

We develop a quantitative analytical treatment of two-point velocity correlations for two important classes of superfluid excitation in compressible quantum fluids: vortices, and rarefaction pulses. We achieve this using two approaches. First, we introduce a new ansatz for describing vortex cores in planar quantum fluids with improved analytic integrability that provides analytic results for power spectra and velocity correlations for general vortex distributions, in good agreement with numerical results using the exact vortex shape. The results show signatures of short and long range correlations associated with vortex dipoles and vortex pairs respectively. Second, for the fast rarefaction pulse regime of the Jones-Roberts soliton the asymptotic high velocity wavefunction provides analytical results for the velocity power spectrum and correlation function, capturing the main length scale of the soliton. We compare our analytical treatment of the homogeneous system with numerical results for a trapped system, finding good quantitative agreement. Our results are relevant to experimental work to characterize quantum vortices and solitons in quantum fluids of atoms and light, and for studies of quantum turbulence.

I. INTRODUCTION

Compressible quantum fluids such as atomic Bose-Einstein condensates [1] (BECs), polariton BEC [2], or quantum fluids of light [3] (QFL) can support quantum vortices [4–7] with finite core scale, and rarefaction pulses that move as solitary waves [8, 9], among other excitations, including Bogoliubov quasiparticles [10]. In planar systems vortices can store significant energy by bunching together, exhibiting negative temperature [11–13]. Beyond the s-wave interacting scalar BEC, spinor BEC [14], spin-orbit coupling [15], and dipolar interactions [16] generate quantum fluids with rich properties such as anisotropic superfluidity [17, 18], and supersolidity [19].

Several experimental measures are used to characterize atomic BECs, and a range of techniques are employed to analyse experiment and simulation data. Experiments including time of flight absorption imaging to approximate the momentum distribution [1], interference [20], and Bragg spectroscopy [21]. However the simultaneous measurement of the density and phase of the BEC order parameter is ruled out by atom number conservation. Furthermore, while Bragg scattering can yield vortex locations and charges [22], technical challenges have limited its widespread adoption. Kinetic energy analysis based on a Helmholtz decomposition of a weighted velocity field [23] has proven invaluable in theoretical studies of compressible quantum turbulence, allowing singularity-free separation of compressible, incompressible, and quantum pressure components of the fluid kinetic energy [24, 25]. However, due to limited density and velocity information this analysis has not been applied to BEC experiments. In contrast, in QFL high resolution density and phase information is directly accessible [26], opening the door to new measurements of superfluid dynamics [27].

Two useful and complimentary measures are power spectra, and their corresponding two-point correlation functions. A commonly used example is the momentum spectrum, integrated over angle in momentum space. When suitably Fourier

transformed this yields the system-averaged first order correlation function of the order parameter [28]. Power spectra for compressible and incompressible kinetic energies are similarly connected with their corresponding two-point correlation functions [25]. These quantities are useful for characterizing the length scales of excitations in the fluid, and can be used as signatures of vortices, rarefaction pulses, and other excitations, and for understanding the physical origins of power-law behavior in quantum turbulence [29]

Power-law signatures of turbulence have a long history. Building on Kolmogorov’s celebrated work [30] on the Richardson cascade in classical turbulence, Novikov derived power-law solutions of the chiral point vortex model relevant to a turbulent energy cascade in a quantum fluid [31]. The analysis also predicts a power law for the velocity two-point correlation function, and was also extended to neutral point vortex systems [32]. While spectral representations can be useful for identifying power laws in turbulent or other scale invariant states, in the absence of power laws there are often well-defined length scales in the system identifiable in real space. In this situation the Fourier transform of the velocity power spectrum provides a system averaged, two-point velocity correlation function [33]. The velocity correlations associated with excitations such as distributions of vortices and rarefaction pulses can shed light on general properties of quantum fluids, and of quantum turbulent states [12, 13, 29, 34, 35].

Theoretical treatment of compressible vortices is complicated by the vortex core structure [24, 36, 37]. Despite some progress in spectral representation [24], the commonly used vortex core ansatz [36] limits analytical results. In particular, an inversion of vortex spectra back to position space to find correlation functions [25] is not known analytically. In a recent experimental and theoretical work the velocity correlation function of compressible and incompressible excitations in a quantum fluid of light were studied in detail [33], enabled by high resolution measurements and spectral analysis [25], and a new analytical approach to the vortex core.

In this paper we introduce an exponential ansatz for the vortex core of a Gross-Pitaevskii fluid, and establish a number of

* ashton.bradley@otago.ac.nz

useful properties in the Fourier domain. We use it to construct velocity power spectra and two-point correlation functions for general vortex distributions in the homogeneous fluid, including a finite size cutoff. The ansatz has improved analytical integrability properties in 2D, yielding analytical results for velocity correlations first presented in [33]. We also consider the rarefaction pulse regime of the Jones–Roberts soliton [8, 38], a localized excitation of density and phase that transports linear momentum at a constant velocity, forming the high velocity counterpart of a vortex dipole. We derive an analytical expression for the velocity correlation function of the rarefaction pulse in the high velocity regime [38, 39]. We compare the vortex and rarefaction pulse results for the homogeneous system to numerical results for a system confined by a harmonic trap. The velocity correlation function gives a clear signature of length scales associated with these compressible and incompressible excitations, providing a useful tool for characterizing quantum fluids.

II. BACKGROUND

A. Gross-Piteavskii equation

We consider a system described by the Gross-Piteavskii equation (GPE) in 2D

$$i\hbar \frac{\partial \psi(\mathbf{r}, t)}{\partial t} = \left(-\frac{\hbar^2}{2m} \nabla^2 + V(\mathbf{r}) + g|\psi(\mathbf{r}, t)|^2 \right) \psi(\mathbf{r}, t), \quad (1)$$

where $\psi(\mathbf{r}, t)$ is the complex wavefunction, $V(\mathbf{r})$ is the external potential, and g is the two-body interaction strength. We consider the homogeneous system, $V(\mathbf{r}) = 0$, and the fluid is in the superfluid phase, with a condensate wavefunction $\psi(\mathbf{r}, t) = \sqrt{n(\mathbf{r}, t)} e^{i\Theta(\mathbf{r}, t)}$. The density $n(\mathbf{r}, t) = |\psi(\mathbf{r}, t)|^2$ and the velocity field $\mathbf{v}(\mathbf{r}, t) = \hbar/m \nabla \Theta(\mathbf{r}, t)$. This system supports quantum vortices, which are topological defects in the phase of the wavefunction [40] that carry angular momentum. It also supports rarefaction pulses, which are compressible solitary waves that move at a constant velocity [8, 41] and carry linear momentum.

A homogeneous system with background density n_0 has natural length unit given by the healing length ξ , related to chemical potential μ and speed of sound c via

$$\mu = gn_0 = \frac{\hbar^2}{m\xi^2} = mc^2. \quad (2)$$

B. Quantum vortices

Vorticity is quantized for the single-valued wavefunction, and the circulation around any closed path C is given by

$$\oint_C \mathbf{v} \cdot d\mathbf{r} = \frac{\hbar}{m} \oint_C \nabla \Theta \cdot d\mathbf{r} = \frac{h}{m} q, \quad (3)$$

where $q = \pm 1$ is the circulation quantum. The vortex velocity field is

$$\mathbf{v}(\mathbf{r}) = \frac{\hbar}{mr} \begin{pmatrix} -\sin \theta \\ \cos \theta \end{pmatrix}, \quad (4)$$

and this field is curl free except precisely at the vortex core, where $\nabla \times \mathbf{v}(\mathbf{r}) = 2\pi q \delta(\mathbf{r})$. The vortex core is a region of suppressed density where the phase winds by 2π , and the core size is of order the healing length ξ . In general the exact vortex core shape must be found numerically [36].

C. Vortex core shape ansatz

A vortex wavefunction that has been useful for evaluating many properties of vortices [36] including energy spectra is given by the ansatz

$$\psi_a(\mathbf{r}) \equiv \sqrt{n_0} \frac{r}{\sqrt{r^2 + (\xi/\Lambda)^2}} e^{\pm i\theta}, \quad (5)$$

where

$$\Lambda = \lim_{r \rightarrow 0} \frac{d}{d(r/\xi)} \log \psi_v(\mathbf{r}) = 0.8249 \dots, \quad (6)$$

is the slope of the exact vortex wavefunction at the core [24]. This ansatz reproduces the correct slope at the origin, and the correct asymptotic behaviour at small and large radii, and the correct vortex velocity field. It has been used to study many properties of quantum vortices in BEC [24, 37, 40, 42].

D. Rarefaction pulse

The Jones–Roberts soliton is a compressible solitary wave solution of the GPE that moves at a constant velocity v [8]. For $0.8c \lesssim v \lesssim c$ it has the asymptotic form [43]

$$n(\mathbf{r}) = n_0 \left(1 - 4\epsilon^2 \frac{3/2 + 2(\epsilon^2 y/\xi)^2 - 2(\epsilon x/\xi)^2}{[3/2 + 2(\epsilon^2 y/\xi)^2 + 2(\epsilon x/\xi)^2]^2} \right), \quad (7)$$

$$\Theta(\mathbf{r}) = -2\sqrt{2}\epsilon \frac{\sqrt{2}\epsilon x/\xi}{3/2 + 2(\epsilon^2 y/\xi)^2 + 2(\epsilon x/\xi)^2}, \quad (8)$$

where $\epsilon = \sqrt{1 - (v/c)^2}$ and c is the speed of sound in the fluid. The density $n(\mathbf{r})$ and phase $\Theta(\mathbf{r})$ describe the rarefaction pulse regime of a Jones–Roberts soliton, with factors of $\sqrt{2}$ due to our definition of ξ .

E. Velocity power spectrum

The velocity power spectrum of a compressible quantum fluid in two dimensions is

$$E(k) = \frac{m}{2} k \int_0^{2\pi} d\phi \left[|\mathcal{F}[\sqrt{n}v_x](\mathbf{k})|^2 + |\mathcal{F}[\sqrt{n}v_y](\mathbf{k})|^2 \right], \quad (9)$$

where

$$\mathcal{F}[f](\mathbf{k}) = \frac{1}{2\pi} \int d^2\mathbf{r} e^{-i\mathbf{k}\cdot\mathbf{r}} f(\mathbf{r}), \quad (10)$$

is the Fourier transform. The density weighted velocity field is used to define the power spectrum for a compressible fluid as it is required to regularize the velocity singularity at a vortex core. The vector field $\mathbf{u}(\mathbf{r}) \equiv \sqrt{n(\mathbf{r})}\mathbf{v}(\mathbf{r})$ may be further decomposed into its compressible (curl free) and incompressible (divergence free) components using a Helmholtz decomposition, $\mathbf{u}(\mathbf{r}) = \mathbf{u}^c(\mathbf{r}) + \mathbf{u}^i(\mathbf{r})$, where $\nabla \cdot \mathbf{u}^i = 0$ and $\nabla \times \mathbf{u}^c = 0$.

F. Vortex power spectrum

In general we can define

$$\psi(\mathbf{r}) \equiv \sqrt{n_0} \chi(r/\xi) e^{\pm i\theta}. \quad (11)$$

For any core shape $\chi(r/\xi)$, assuming a pure azimuthal velocity field, to determine the power spectrum, we want to find the two dimensional Fourier transform of

$$\mathbf{u}(\mathbf{r}) = \sqrt{n(\mathbf{r})}\mathbf{v}(\mathbf{r}) = \frac{\hbar \sqrt{n_0} \chi(r/\xi)}{m} \begin{pmatrix} -\sin \theta \\ \cos \theta \end{pmatrix} \quad (12)$$

We can write this as

$$\begin{aligned} \tilde{\mathbf{u}}(\mathbf{k}) &\equiv \frac{1}{2\pi} \int d^2\mathbf{r} e^{-i\mathbf{k}\cdot\mathbf{r}} \mathbf{u}(\mathbf{r}) \\ &= \frac{\hbar \sqrt{n_0}}{m} \int_0^\infty dr \chi(r/\xi) \frac{1}{2\pi} \int_0^{2\pi} d\theta e^{ikr \cos(\theta-\phi)} \begin{pmatrix} -\sin \theta \\ \cos \theta \end{pmatrix} \end{aligned} \quad (13)$$

where ϕ is the angle \mathbf{k} makes to the x axis. Using the Bessel function identity

$$\frac{1}{2\pi} \int_0^{2\pi} d\theta e^{ikr \cos(\theta-\phi)} \begin{pmatrix} -\sin \theta \\ \cos \theta \end{pmatrix} = iJ_1(kr) \begin{pmatrix} -\sin \phi \\ \cos \phi \end{pmatrix}, \quad (14)$$

and, provided $k > 0$ we have

$$J_1(kr) = -\frac{1}{k} \frac{dJ_0(kr)}{dr}. \quad (15)$$

We can integrate by parts and change variables to find

$$\tilde{\mathbf{u}}(\mathbf{k}) = \frac{i\hbar \sqrt{n_0}}{mk} \int_0^\infty d\sigma \chi'(\sigma) J_0(k\xi\sigma) \begin{pmatrix} -\sin \phi \\ \cos \phi \end{pmatrix}, \quad (16)$$

a convenient form, since $\chi'(\sigma) \rightarrow 0$ as $\sigma \rightarrow \infty$. The incompressible velocity power spectrum is now found as

$$E(k) = \frac{m}{2} k \int_0^{2\pi} d\phi |\tilde{\mathbf{u}}(\mathbf{k})|^2 = e_0 \xi F(k\xi), \quad (17)$$

where

$$F(z) \equiv \frac{1}{z} \left(\int_0^\infty d\sigma \chi'(\sigma) J_0(\sigma z) \right)^2, \quad (18)$$

and

$$e_0 \equiv \frac{\pi \hbar^2 n_0}{m} = \pi \mu n_0 \xi^2 \quad (19)$$

is the energy unit. In this form we can consider different ansatz for single or multiply charged cores, dipolar vortices, etc.

The function $F(z)$ has the following asymptotic properties:

- (i) Point vortex limit: $F(z) \rightarrow 1/z$ for $z \ll 1$, independent of the particular core shape. This follows since χ' is only nonzero over a small range of $\sigma \lesssim 10$, and so for small z , $J_0(\sigma z) \simeq J_0(0) = 1$ and may be taken outside the integral. Since $\chi(0) = 0$ and $\chi(\infty) = 1$ we have

$$\int_0^\infty \chi'(\sigma) d\sigma = -1. \quad (20)$$

- (ii) Vortex core limit: $F(z) \rightarrow \Lambda^2/z^3$ for $z \gg 1$. This follows from the change of variables $u = \sigma z$, giving

$$\int_0^\infty d\sigma \chi'(\sigma) J_0(\sigma z) = \frac{1}{z} \int_0^\infty du \chi'(u/z) J_0(u) \rightarrow \frac{\chi'(0)}{z}, \quad (21)$$

since $\int_0^\infty du J_0(u) = 1$.

III. VORTICES

A particular form of the spectrum was calculated using the rational ansatz in [24]. It had the correct UV and IR asymptotics, but the mid range involved a product of Bessel functions, limiting further analytical work. In this section we calculate the velocity power spectrum and two-point velocity correlation function for a system of compressible quantum vortices in a homogeneous fluid. For this purpose we introduce a new ansatz for the vortex core that simplifies the calculation of the power spectrum and velocity correlations for general vortex distributions.

A. Exponential ansatz

For the purpose of analytical work, we seek a description of the compressible fluid vortex core that is more tractable than the rational ansatz. The key property we seek is the simplest Fourier transform, with the final aim that a Fourier inversion can be performed analytically to find the two-point velocity correlation function.

We introduce the following exponential ansatz

$$\psi_e(\mathbf{r}) \equiv \sqrt{n_0} (1 - e^{-\Lambda r/\xi}) e^{\pm i\theta}. \quad (22)$$

It has the vortex slope at the origin, and also approaches the correct asymptotic for a GPE vortex at large radii. This is compared with the rational ansatz and the exact core shape in Fig. 1. We note that the exponential ansatz converges to the exact far field density more rapidly than the rational ansatz. However, the core shape is not as accurate, but approaches the correct slope Λ/ξ for $r \ll \xi$.

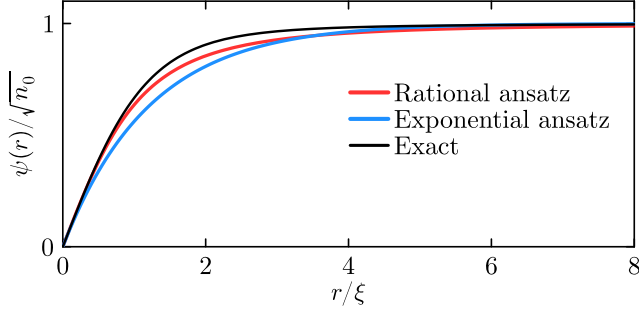


FIG. 1. Comparison of the vortex core ansatz with the exact core shape. The black line shows the numerically exact core solution for the two-dimensional Gross-Pitaevskii equation. The blue line shows the exponential ansatz (23), and the red line shows the rational ansatz (5).

B. Vortex power spectrum

For the exponential ansatz

$$\chi_e(\sigma) \equiv (1 - e^{-\Lambda\sigma}) \quad (23)$$

and to evaluate Eq. (18) for this core shape, we use (B1) to find

$$\int_0^\infty d\sigma \chi'_e(\sigma) J_0(\sigma z) = \frac{\Lambda}{\sqrt{z^2 + \Lambda^2}}, \quad (24)$$

and consequently the spectral function

$$F_\Lambda(z) = \frac{\Lambda^2}{z(z^2 + \Lambda^2)} = \frac{1}{z} - \frac{z}{z^2 + \Lambda^2}. \quad (25)$$

This representation of the vortex core transform has properties $F_\Lambda(z) \rightarrow 1/z$ as $z \rightarrow 0$, and $F_\Lambda(z) \rightarrow \Lambda^2/z^3$ as $z \rightarrow \infty$, giving spectrum

$$E^i(k) = e_0 \xi F_\Lambda(k\xi), \quad (26)$$

with a point-vortex term dominant at wavenumbers $2\pi/R \ll k \ll 2\pi/\xi$, and a core contribution evident for large wavenumbers $k \gg 2\pi/\xi$, as shown in Fig. 2 (a).

C. Two-point velocity correlation function

A useful measure of the velocity field is the two-point velocity correlation function, which describes the correlation between the velocity field at two points separated by a distance r . The point-wise correlation is averaged over the system to give a global statistical measure of the velocity field correlation length scales. The correlation function is also calculated as the Fourier transform of the velocity power spectrum.

In detail, the two-point velocity correlation function between two vector fields is defined as

$$C[\mathbf{u}, \mathbf{v}](\mathbf{r}) \equiv \int d^2\mathbf{R} \mathbf{u}^*(\mathbf{R} - \mathbf{r}/2) \cdot \mathbf{v}(\mathbf{R} + \mathbf{r}/2) \quad (27)$$

and we are interested in the angle-averaged autocorrelation function

$$G(r) \equiv \frac{1}{2\pi} \int_0^{2\pi} d\theta C[\mathbf{u}, \mathbf{u}](r \cos \theta, r \sin \theta). \quad (28)$$

This two-point velocity correlation may also be calculated via the inverse Fourier transform of the velocity power spectrum [44], as the integral [25]

$$G(r) = \int_0^\infty dk E(k) J_0(kr). \quad (29)$$

The simplicity of the expression (26) allows us to evaluate $G(r)$ for a system of quantum vortices within the exponential ansatz, using (25), (26),

$$\begin{aligned} G_\Lambda^i(r) &= e_0 \xi \int_0^\infty dk F(k\xi) J_0(kr) \\ &= e_0 \int_0^\infty dz J_0(zr/\xi) \left(\frac{1}{z} - \frac{z}{z^2 + \Lambda^2} \right). \end{aligned} \quad (30)$$

The second term can be easily evaluated using (B2), however, in the first term there is an apparent divergence at $z = 0$ due to the long range velocity field of the vortex. Fortunately, there is a regularized form of the point vortex integral that allows progress:

$$\int_0^\infty dz \frac{1}{\sqrt{z^2 + \Gamma^2}} J_0(zx) = I_0\left(\frac{\Gamma x}{2}\right) K_0\left(\frac{\Gamma x}{2}\right), \quad (31)$$

where $\Gamma = 2\pi/\bar{R} \ll 1$ is an infrared cutoff for system size $\bar{R} = R/\xi \gg 1$. We introduce the regularized form $F_\Lambda(z) \rightarrow F_e(z)$ for the exponential ansatz, defined as

$$F_e(z) \equiv \frac{1}{\sqrt{z^2 + \Gamma^2}} - \frac{z}{z^2 + \Lambda^2}, \quad (32)$$

corresponding to the single vortex spectrum

$$E_e^i(k) = e_0 \xi F_e(k\xi). \quad (33)$$

The net effect is to remove the infrared divergence in the velocity field of the vortex, as shown in Fig. 2 (a). Carrying out the inversion integral (29), we find the two-point correlator

$$G_e^i(r) = e_0 \left(K_0\left(\frac{\Gamma r}{2\xi}\right) I_0\left(\frac{\Gamma r}{2\xi}\right) - K_0\left(\frac{\Lambda r}{\xi}\right) \right). \quad (34)$$

Since $K_0(x)I_0(x) - K_0(ax) \rightarrow \ln(a)$ as $x \rightarrow 0$, we have the normalized incompressible velocity correlation function for a single vortex in the form

$$g_e^i(r) \equiv \frac{G_e^i(r)}{G_e^i(0)} = \frac{K_0\left(\frac{\Gamma r}{2\xi}\right) I_0\left(\frac{\Gamma r}{2\xi}\right) - K_0\left(\frac{\Lambda r}{\xi}\right)}{\ln\left(\frac{2\Lambda}{\Gamma}\right)}, \quad (35)$$

shown in Fig. 2 (b). The singular behavior at the origin in the first term is removed by the second term, reliant on the separation of scales $\Gamma \ll \Lambda$, equivalent to $\xi \ll R$, always valid in the point-vortex regime where the background superfluid density is large. For $z \gg 1$, the second term is exponentially suppressed and $I_0(z)K_0(z) \rightarrow 1/(2z)$ at leading order, and hence the correlator decay is akin to that of the single-vortex velocity field.

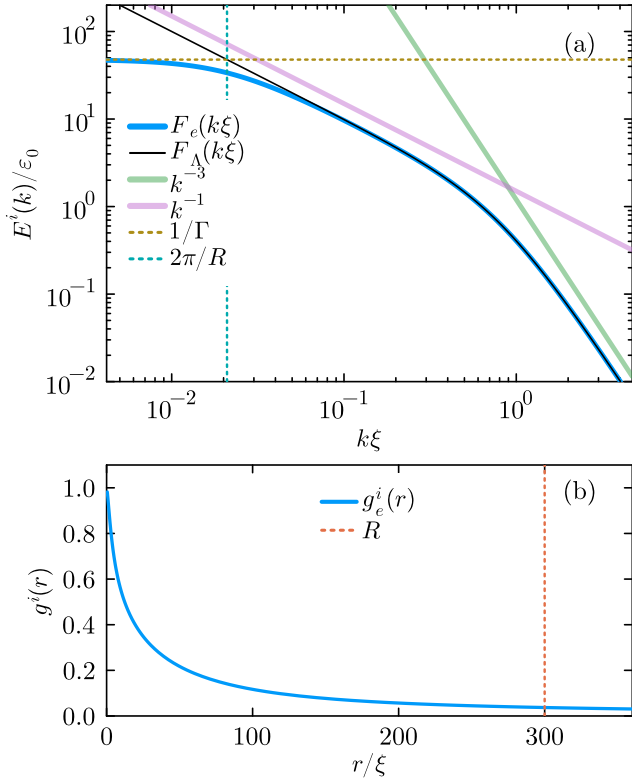


FIG. 2. Single vortex properties. (a) Incompressible velocity power spectrum. Blue curve shows the IR regularized exponential for $R = 300\xi$. Spectrum shows the expected vortex power laws for the near and far field, until $k\xi \sim \Gamma = 2\pi/R$ where it flattens due to the infrared regularisation. (b) Normalized two-point velocity correlation for the exponential ansatz, corresponding to the spectrum in (a).

D. Vortex distributions

A system of N well-separated vortex cores with sign of circulation q_i and position \mathbf{r}_i has generalised velocity field

$$\mathbf{u}(\mathbf{r}) = \sum_{i=1}^N q_i \mathbf{u}_s(\mathbf{r} - \mathbf{r}_i), \quad (36)$$

where $\mathbf{u}_s(\mathbf{r})$ is the single vortex velocity field (12). The construction is additive due to the additivity of the quantum phase for vortices in a homogeneous background, and the separation of vortex cores ensuring that the core profiles are independent. The incompressible velocity power spectrum is then found by evaluating (9) to find [24]

$$E^i(k) = e_0 \xi F_e(k\xi) \sum_{i=1, j=1}^N q_i q_j J_0(k|\mathbf{r}_i - \mathbf{r}_j|). \quad (37)$$

To calculate the two-point velocity correlator (29) we need to evaluate the integral

$$U(a, b) \equiv \int_0^\infty dz F_e(z) J_0(za) J_0(zb). \quad (38)$$

We evaluate this integral in Appendix A, arriving at the result

$$U(a, b) = I_0\left(\frac{\Gamma\alpha}{2}\right) K_0\left(\frac{\Gamma\alpha}{2}\right) - I_0(\Lambda\beta) K_0(\Lambda\alpha) \quad (39)$$

where $\alpha \equiv \max(a, b)$ and $\beta \equiv \min(a, b)$. This enables a singularity-free construction of the two-point velocity correlator for a general multivortex system. Note that $U(a, b) = U(b, a)$.

The general two-point correlator can now be written as

$$G^i(r) = e_0 \xi \sum_{i=1, j=1}^N q_i q_j U(r/\xi, r_{ij}/\xi). \quad (40)$$

where $r_{ij} = |\mathbf{r}_i - \mathbf{r}_j|$. Same and opposite sign vortices contribute differently to the correlations. The normalized correlator reads

$$g^i(r) = \frac{1}{\sum_{i=1, j=1}^N q_i q_j U(0, r_{ij}/\xi)} \sum_{i=1, j=1}^N q_i q_j U(r/\xi, r_{ij}/\xi), \quad (41)$$

and has the properties:

1. $g^i(0) = 1$ by construction.
2. For a single vortex we recover the correct expression (34).
3. For $r \ll r_{ij}$, the correlator is dominated by the universal core contribution, and the point vortex far field is not relevant.
4. For $r \gg r_{ij}$, the point vortex far field dominates, and the total charge of the vortex distribution is relevant.

E. Incompressible approximation

Thus far our analysis is essentially exact, due to the accuracy of asymptotics used. Our aim is to retain the main compressible effects for $r \ll \xi$, but neglect the small compressible corrections around vortex cores at large distances. This will greatly simplify the analytical results.

For the point vortex regime of well-separated vortices, since $\Lambda = 0.8249\dots$, we always have $\Lambda r_{ij} \gg \xi$, and hence when $a \ll b$, we have $(\alpha, \beta) = (b, a)$, and it will be an excellent approximation in general that

$$U(a, b) \simeq \tilde{U}(a, b) \equiv I_0\left(\frac{\Gamma\alpha}{2}\right) K_0\left(\frac{\Gamma\alpha}{2}\right) - K_0(\Lambda\alpha), \quad (42)$$

provided $r_{ij} \gg \xi$. We refer to this as the incompressible approximation. The validity may be understood as a consequence of $\Gamma \ll \Lambda$, or $\xi \ll R$, as follows. On the face of it, one may guess that this is due to $I_0(x) \rightarrow 1$ for small arguments. However, it is valid more broadly as the second term is only a small correction to the first at large arguments due to its asymptotic suppression.

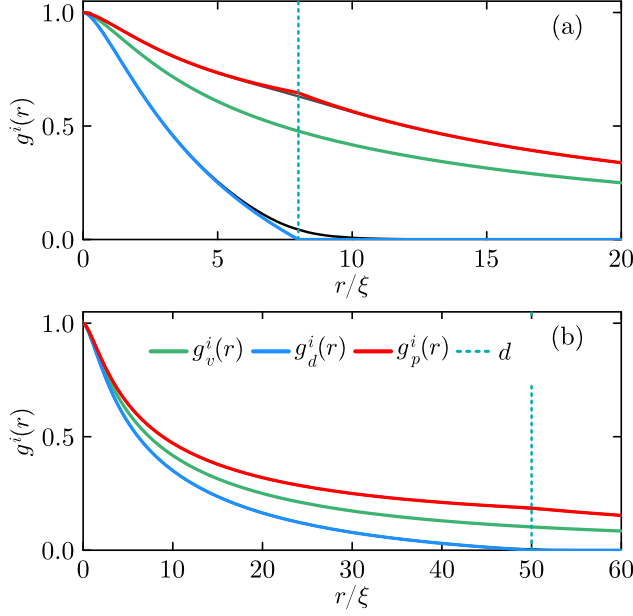


FIG. 3. Two-point correlation functions of the incompressible velocity. The black lines show the (essentially exact) correlation function (41), and the colored lines show the approximate forms for a single vortex (43), a vortex dipole (44), and a pair of same-sign vortices (45). (a) $d = 8\xi$, (b) $d = 50\xi$. For the infrared cutoff $\Gamma = 2\pi/R$ we set $R = 56\xi$ for both plots.

F. Few vortex states

We now consider some simple cases for which we have an analytical approach.

Single vortex.— A single vortex has two-point incompressible velocity correlator

$$g_v^i(r) \equiv \frac{K_0\left(\frac{\Gamma r}{2\xi}\right)I_0\left(\frac{\Gamma r}{2\xi}\right) - K_0\left(\frac{\Lambda r}{\xi}\right)}{\ln\left(\frac{2\Lambda}{\Gamma}\right)}. \quad (43)$$

Vortex Dipole.— A pair of vortices of opposite sign separated by d has correlator

$$g_d^i(r) = \begin{cases} \frac{g_v^i(r) - g_v^i(d)}{1 - g_v^i(d)}, & r \leq d \\ 0, & r > d. \end{cases} \quad (44)$$

Vortex Pair.— A pair of same sign vortices separated by d has correlator

$$g_p^i(r) = \begin{cases} \frac{g_v^i(r) + g_v^i(d)}{1 + g_v^i(d)}, & r \leq d \\ \frac{2g_v^i(r)}{1 + g_v^i(d)}, & r > d. \end{cases} \quad (45)$$

Example velocity correlations for the vortex, dipole, and pair are shown in Fig. 3. In (a) we show a small vortex separation, and in (b) a large separation. In contrast to the long range

behavior of a single vortex, the dipole has velocity correlation that drops to zero near the separation scale d , corresponding to the significant cancellation of velocity at larger distances [45]. The vortex pair on the other hand has enhanced velocity correlation at short scales and at large scales decays like a charge 2 single vortex. Compressible effects are evident for (a) near the separation scale d , but are negligible in (b) where $\xi \ll d$.

Relative to the single vortex, the vortex pair correlator at $r = d$ is enhanced by the factor $1 < 2/(1 + g_v^i(d)) \leq 2$, due to the superposition of the two corotating vortex fields, as shown in (a) and (b). For larger d , the enhancement saturates near a factor of 2, as shown in (b).

IV. RAREFACTION PULSE

At leading order $\sqrt{n}v_x \approx \sqrt{n_0}v_x$, i.e. the background density variations do not matter at leading order for a fast rarefaction pulse, and our aim is to understand the velocity field. In terms of the quantum phase, this takes the form

$$\sqrt{n_0}v_x = \frac{\sqrt{n_0}\hbar}{m}(-2\sqrt{2}\epsilon)\partial_x \frac{\sqrt{2}\epsilon x/\xi}{3/2 + 2(\epsilon x/\xi)^2 + 2(\epsilon^2 y/\xi)^2} \quad (46)$$

The Fourier transform can then be written as

$$\begin{aligned} \mathcal{F}[\sqrt{n_0}v_x] &= \frac{\sqrt{n_0}\hbar}{m}(-2\sqrt{2}\epsilon)ik_x \\ &\times \frac{1}{2\pi} \int d^2\mathbf{r} e^{-i\mathbf{k}\cdot\mathbf{r}} \frac{\sqrt{2}\epsilon x/\xi}{3/2 + 2(\epsilon x/\xi)^2 + 2\epsilon^2(\epsilon y/\xi)^2}. \end{aligned} \quad (47)$$

We can try to proceed exactly, but the anisotropy means that the integral $\int d\theta_k$ cannot be evaluated. We have identified a simple approximation that captures the velocity decorrelation length scale at short range: we simply ignore the slower decay in the y direction, setting $\epsilon^2 \rightarrow 1$ in the denominator [46]. This approximates the denominator as cylindrically symmetric:

$$\begin{aligned} \mathcal{F}[\sqrt{n_0}v_x] &\approx \frac{\sqrt{n_0}\hbar}{m}(-2\sqrt{2}\epsilon)ik_x \\ &\times \frac{1}{2\pi} \int d^2\mathbf{r} e^{-i\mathbf{k}\cdot\mathbf{r}} \frac{\sqrt{2}\epsilon x/\xi}{3/2 + 2(\epsilon x/\xi)^2 + 2(\epsilon y/\xi)^2}, \end{aligned} \quad (48)$$

but retains the dominant anisotropy due to the phase jump in the x direction. This approximation captures well the main length scale of the velocity correlation function we are interested in.

Changing variables $\sqrt{2}\epsilon x/\xi = \sqrt{3/2}u$, $\sqrt{2}\epsilon y/\xi = \sqrt{3/2}v$, we have $dx dy = (3/2)\xi^2/(2\epsilon^2)dudv$, and the integral becomes

$$\begin{aligned} \mathcal{F}[\sqrt{n_0}v_x] &\approx \frac{\sqrt{n_0}\hbar}{m}(-\sqrt{3}\xi^2/\epsilon)ik_x \\ &\times \frac{1}{2\pi} \int dudv e^{-i(k_x u + k_y v)\xi\sqrt{3}/(2\epsilon)} \frac{u}{1 + u^2 + v^2}. \end{aligned} \quad (49)$$

By first doing the polar integral using (B7), the integral can be evaluated to give

$$\mathcal{F}[\sqrt{n_0}v_x] \simeq i \frac{\sqrt{n_0}\hbar}{m} \frac{\sqrt{3}\xi^2}{\epsilon} \frac{k_x^2}{k} K_1(k\lambda/2), \quad (50)$$

$$\mathcal{F}[\sqrt{n_0}v_y] \simeq i \frac{\sqrt{n_0}\hbar}{m} \frac{\sqrt{3}\xi^2}{\epsilon} \frac{k_x k_y}{k} K_1(k\lambda/2). \quad (51)$$

where $\lambda \equiv \sqrt{3}\xi/\epsilon$ turns out to be the scale of the angle-integrated velocity correlation function. In this approximation, the (compressible) energy spectrum (9) is

$$E^c(k) = e_0\xi \frac{3}{2\epsilon^2} (k\xi)^3 K_1(k\lambda/2)^2. \quad (52)$$

The two-point correlator is

$$\begin{aligned} G(r) &= \int_0^\infty dk E(k) J_0(kr) = e_0\xi^4 \frac{3}{2\epsilon^2} \\ &\times \int_0^\infty dk k^3 J_0(kr) K_1(k\lambda/2)^2 \\ &= e_0\xi^2 \int_0^\infty dz z^3 J_0(zr/\lambda) K_1(z/2)^2 \end{aligned} \quad (53)$$

where we changed to $z = k\lambda$. Making use of integral (B8), we find the normalized correlator $g^c(r) = G(r)/G(0) \equiv f(r/\lambda)$, where

$$f(x) = \frac{3}{8(x^2 + 1)^2} \left(1 - \frac{1}{2x^2} + \frac{2(x^2 + 1/4)}{x^3 \sqrt{x^2 + 1}} \operatorname{csch}^{-1} \left(\frac{1}{x} \right) \right). \quad (54)$$

This function, and its dependence on r/λ , captures the key length scale of rarefaction pulse velocity correlations. An example is shown in the following section which also examines the effect of a background density gradient. For the localized structures of dipole and rarefaction pulse the background variation effect is minimal when the background is locally slowly varying.

It is worth noting that although the rarefaction pulse wavefunction has a lower velocity limit of $v \simeq 0.8c$ for physical validity (positive density), there is no such limit on the two point correlation function (54). This property was recently used to characterize correlations near the point of rarefaction pulse formation [33].

V. TRAPPED SYSTEM

An inhomogenous background density is more commonly encountered in experiments, both in BECs and photon quantum fluids [3, 26]. It is worthwhile to consider the role of background curvature of the quantum fluid density, and the new scale introduced by the system size. We consider a harmonic trap with frequency ω_\perp , and work in units of the oscillator length $a_\perp = \sqrt{\hbar/m\omega_\perp}$. The system consists of a BEC with chemical potential $\mu = 40\hbar\omega_\perp$, with healing length $\xi = 0.158a_\perp$, and Thomas-Fermi radius $R = \sqrt{2\mu/m\omega_\perp} = 56.6a_\perp$. We use a numerical grid of $(n_x, n_y) = (512, 512)$ points, over a

square domain of side length $5R$ to represent the trapped system as a Thomas-Fermi ground state. In trap units, the dimensionless interaction strength $g = 0.1$ corresponds to a system of $N_a = 5 \times 10^4$ atoms.

Velocity power spectra and correlations are calculated numerically using the high resolution Fourier method described in [25]. In essence, the problem of binning on coarse momentum grids is avoided by doing the angular integral in momentum space analytically. Each point in the numerical spectrum then requires a forward and inverse Fourier transform to complete, gaining flexibility and accuracy (especially for low k) in the spectrum. High resolution allows accurate numerical evaluation of (29). The incompressible velocity power spectra are shown in Fig. 4 for a single vortex, a pair of vortices, a vortex dipole, and a rarefaction pulse with $v = 0.85c$. The velocity correlation functions are shown in Fig. 5. For vortices, the characteristics are akin to Fig. 3, with finite size effects now evident at small k , corresponding to different long range decay of the velocity correlation at distances of order R ; these differences are only strongly evident for the long-ranged configurations in Fig. 5 (a), (b). For the vortex dipole and rarefaction pulse, Fig. 5 (c), (d), we see the characteristic short range coherence lengths d and λ for compressible and incompressible velocity respectively.

The trapped system results have recently been tested against a high resolution experiment in a quantum fluid of light, finding good quantitative agreement [33], such an analysis is only possible in a quantum fluid of light where the Helmholtz decomposition can be carried out on high resolution density and velocity fields [23, 25].

VI. CONCLUSION

Quantum vortices are a fundamental feature of quantum fluids acquiring rotation. The tension between kinetic and nonlinear energies in determining the core shape means that the exact shape is not known analytically, and certain ansatzes are commonly used to expedite analytical calculations. Aiming to develop a more tractable treatment of vortices, in this work we have introduced a new vortex core ansatz with improved analytical integrability.

We have used the exponential ansatz to solve the general problem of calculating the power spectrum of a planar compressible quantum fluid containing vortices, and Fourier transforming the spectrum gives the two-point velocity correlator for vortex distributions. We further considered simple vortex distributions by identifying an incompressible approximation, revealing signatures of short and long range velocity coherences (vortex dipole and pair respectively), and the associated length scales. The vortex pair has enhanced correlation due to the coherent long range velocity field, while the vortex dipole has velocity correlations that decay to zero over the scale of the vortex separation. Our results for vortices are compared with similar analysis for the rarefaction pulse regime of a Jones-Roberts soliton which also has a characteristic short range velocity coherence length.

The exponential vortex ansatz may have a number of wider

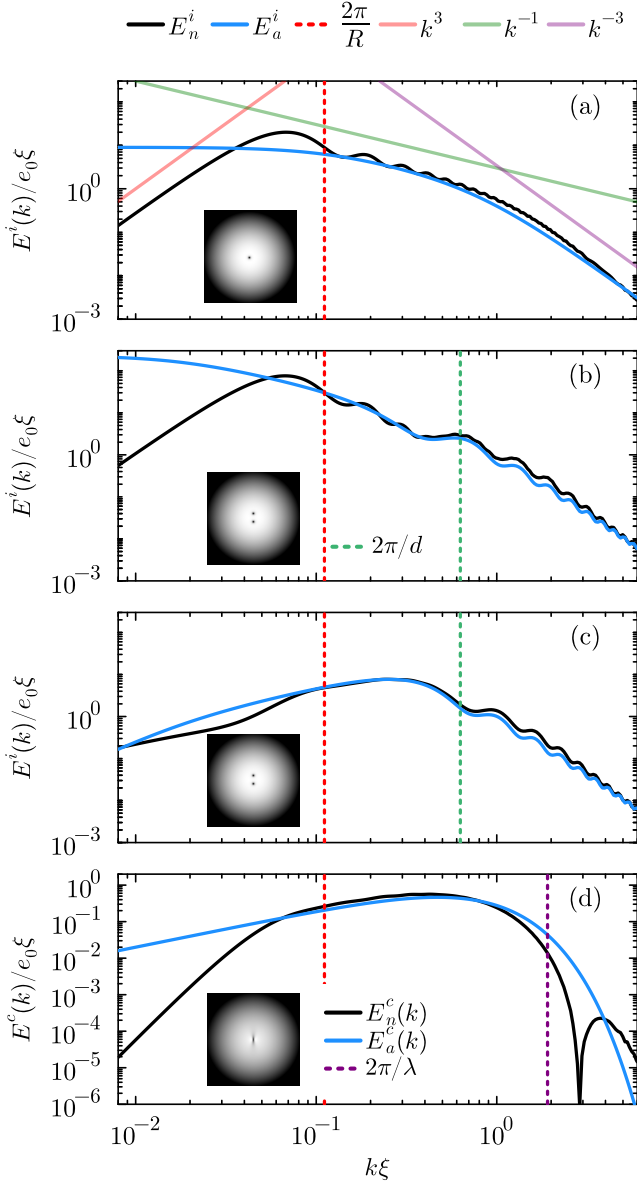


FIG. 4. Energy spectra in a trapped BEC, comparing the numerical spectrum for a Thomas-Fermi state imprinted with (a) a single vortex (density inset), with power laws for comparison; (b) a pair of vortices of the same sign with separation $d = 10\xi$; (c) a vortex dipole with the same separation; (d) Rarefaction pulse with $v = 0.85c$. The numerically calculated spectra, $E_n^{i,c}$ are compared with (37) for (a)-(c), and (52) for (d), where $\lambda = \sqrt{3}\xi/\epsilon$. The analytical expressions are evaluated using an infrared cutoff $\Gamma = 2\pi/R$, and the Thomas-Fermi radius is $R = 56\xi$ for all subplots.

applications in the study of 2D quantum vortex dynamics [37] and quantum turbulence [24]. A future area of interest is the role of dissipative effects in rarefaction pulse dynamics [38], for which velocity correlations could prove a useful characterization. Vortex core changes in dipolar systems [16], and compressible effects in planar quantum turbulence [24, 47, 48] may also be interesting directions for investigation. General-

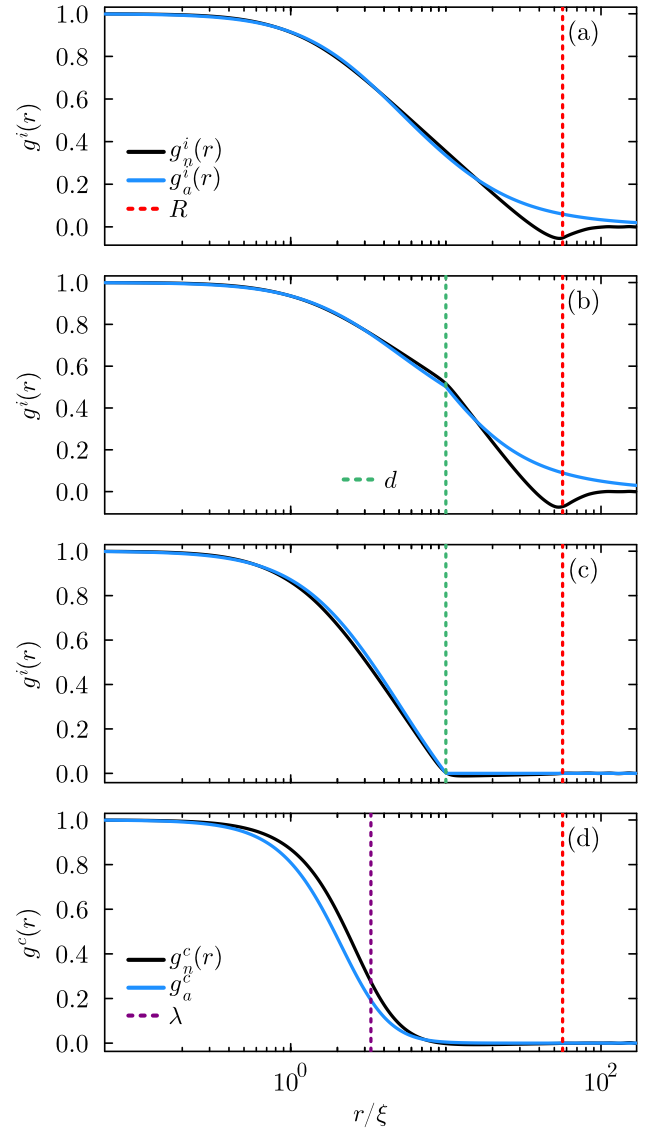


FIG. 5. Angle averaged velocity two point correlation function in a trapped BEC. (a) a single central vortex. (b) a pair of vortices with separation $d = 10\xi$. (c) a vortex dipole with the same separation; (a)-(d) show the incompressible velocity correlation function. (d) a rarefaction pulse with $v = 0.85c$, showing the compressible velocity correlation function, with $\lambda = \sqrt{3}\xi/\epsilon$. The black lines show the numerically calculated correlation function for inhomogeneous system, and the blue lines show the analytical expressions for a homogeneous system with an infrared cutoff $\Gamma = 2\pi/R$, with $R = 56\xi$ for all subplots.

ized point vortex models that include dissipative effects [37] would also benefit from a simpler core ansatz.

ACKNOWLEDGMENTS

AB would like to acknowledge the hospitality of Quentin Glorieux's research group at LKB ENS Sorbonne Université

where this work was initiated. The authors acknowledge the Dodd-Walls Centre for Photonic and Quantum Technologies for financial support.

Appendix A: Correlation integral

To calculate the two-point correlation for vortices we require the integral

$$\begin{aligned} U(a, b) &= \int_0^\infty dz F_e(z) J_0(za) J_0(zb) \\ &= \int_0^\infty dz \left(\frac{1}{\sqrt{z^2 + \Gamma^2}} - \frac{z}{z^2 + \Lambda^2} \right) J_0(za) J_0(zb). \end{aligned} \quad (\text{A1})$$

Note that $U(a, 0) = G_e^i(a)$, and $U(0, 0) = G_e^i(0) = \ln(2\Lambda/\Gamma)$. The second term can be integrated using (B3). This is always well defined since K_0 is always evaluated at the larger argument, avoiding the logarithmic divergence for small arguments.

The first integral

$$I(a, b, \Gamma) = \int_0^\infty dz \frac{J_0(az) J_0(bz)}{\sqrt{z^2 + \Gamma^2}} \quad (\text{A2})$$

is not known in closed form. However, we can evaluate it to a very good approximation as follows. First, we use the Fourier transform (B4) and extend the z integral to the real line

$$I(a, b, \Gamma) = \frac{1}{2\pi} \int_{-\infty}^\infty dk K_0(\Gamma|k|) \int_{-\infty}^\infty dz J_0(az) J_0(bz) e^{ikz}. \quad (\text{A3})$$

Consider the case $a \gg b$, and put $u = az$. Then

$$\begin{aligned} I(a, b, \Gamma) &= \frac{1}{2\pi a} \int_{-\infty}^\infty dk K_0(\Gamma|k|) \int_{-\infty}^\infty du J_0(u) J_0(bu/a) e^{iku/a} \\ &\simeq \frac{1}{\sqrt{2\pi a}} \int_{-\infty}^\infty dk K_0(\Gamma|k|) \int_{-\infty}^\infty du J_0(u) \frac{e^{iku/a}}{\sqrt{2\pi}}. \end{aligned} \quad (\text{A4})$$

Also, we use the Fourier representation of the Bessel function (B5), or the Fourier transform pair

$$J_0(x) \longleftrightarrow \sqrt{\frac{2}{\pi}} \frac{\Pi(k/2)}{\sqrt{1-k^2}}, \quad (\text{A5})$$

where $\Pi(x)$ is the rectangular function of unit width and height. We then have

$$\begin{aligned} I(a, b, \Gamma) &\simeq \frac{1}{\pi a} \int_{-\infty}^\infty dk K_0(\Gamma|k|) \frac{\Pi(k/2a)}{\sqrt{1-(k/a)^2}} \\ &= \frac{2}{\pi} \int_0^1 du \frac{K_0(\Gamma a k)}{\sqrt{1-k^2}}. \end{aligned} \quad (\text{A6})$$

Using the integral (B6) we have

$$I(a, b, \Gamma) = I_0(\Gamma a/2) K_0(\Gamma a/2) \quad \text{for } a \gg b. \quad (\text{A7})$$

The integrand is symmetric in a and b , and we require both limits. Since the two asymptotic results are continuous at $a = b$ we use it for all a, b as a matched asymptotic expansion:

$$I(a, b, \Gamma) = \begin{cases} I_0(\Gamma a/2) K_0(\Gamma a/2) & \text{for } a > b. \\ I_0(\Gamma b/2) K_0(\Gamma b/2) & \text{for } a < b. \end{cases} \quad (\text{A8})$$

Putting it together, we have the transform

$$\begin{aligned} U(a, b) &= \int_0^\infty dz F_\Gamma(z) J_0(za) J_0(zb) \\ &= I(a, b, \Gamma) - \int_0^\infty dz \frac{z}{z^2 + \Lambda^2} J_0(za) J_0(zb) \\ &= \begin{cases} I_0(\Gamma a/2) K_0(\Gamma a/2) - K_0(\Lambda a) I_0(\Lambda b) & \text{for } a > b. \\ I_0(\Gamma b/2) K_0(\Gamma b/2) - K_0(\Lambda b) I_0(\Lambda a) & \text{for } a < b. \end{cases} \end{aligned} \quad (\text{A9})$$

Appendix B: Bessel function integrals

We collect several useful Bessel function integrals and integral representations here for completeness. In some cases these are already tabulated, while others may be less well known.

For working with vortices we use

$$\int_0^\infty e^{-\alpha x} J_\nu(\beta x) dx = \frac{\beta^{-\nu} [\sqrt{\alpha^2 + \beta^2} - \alpha]^\nu}{\sqrt{\alpha^2 + \beta^2}}, \quad (\text{B1})$$

$$\int_0^\infty x^{\nu+1} J_\nu(ax) \frac{dx}{x^2 + b^2} = b^\nu K_\nu(ab), \quad (\text{B2})$$

$$\int_0^\infty \frac{J_0(az) J_0(bz) z}{z^2 + c^2} dz = I_0(\min(a, b)c) K_0(\max(a, b)c), \quad (\text{B3})$$

$$\frac{1}{\sqrt{z^2 + \Gamma^2}} = \frac{1}{\pi} \int_{-\infty}^\infty dk K_0(\Gamma|k|) e^{ikz}, \quad (\text{B4})$$

$$J_0(x) = \frac{1}{\pi} \int_{-1}^1 \frac{e^{ikx}}{\sqrt{1-k^2}} dk, \quad (\text{B5})$$

$$\int_0^1 du \frac{K_0(au)}{\sqrt{1-u^2}} = \frac{\pi}{2} I_0(a/2) K_0(a/2). \quad (\text{B6})$$

For the rarefaction pulse we use the following integrals

$$\frac{1}{2\pi} \int dudv e^{-i(k_x u + k_y v)a} \frac{u}{1+u^2+v^2} = -i K_1(ak) k_x/k, \quad (\text{B7})$$

$$\begin{aligned} \int_0^\infty dk k^3 J_0(ak) K_1(bk/2)^2 &= \frac{4}{a^3(a^2 + b^2)^2} \\ &\times \left(a^3 - \frac{ab^2}{2} + \frac{2b^2(a^2 + b^2/4)}{\sqrt{a^2 + b^2}} \operatorname{csch}^{-1} \left(\frac{b}{a} \right) \right). \end{aligned} \quad (\text{B8})$$

- [1] M. H. Anderson, J. R. Ensher, M. R. Matthews, C. E. Wieman, and E. A. Cornell, Observation of Bose-Einstein Condensation in a Dilute Atomic Vapor, *Science* **269**, 198 (1995).
- [2] H. Deng, G. Weihs, C. Santori, J. Bloch, and Y. Yamamoto, Condensation of Semiconductor Microcavity Exciton Polaritons, *Science* **298**, 199 (2002).
- [3] Q. Fontaine, T. Bienaimé, S. Pigeon, E. Giacobino, A. Bramati, and Q. Glorieux, Observation of the Bogoliubov Dispersion in a Fluid of Light, *Physical Review Letters* **121**, 183604 (2018).
- [4] L. P. Pitaevskii, Vortex lines in an imperfect Bose gas, *Soviet Physics JETP* **13**, 451 (1961).
- [5] M. R. Matthews, B. P. Anderson, P. C. Haljan, D. S. Hall, C. E. Wieman, and E. A. Cornell, Vortices in a Bose-Einstein Condensate, *Physical Review Letters* **83**, 2498 (1999).
- [6] K. W. Madison, F. Chevy, W. Wohlleben, and J. Dalibard, Vortex Formation in a Stirred Bose-Einstein Condensate, *Physical Review Letters* **84**, 806 (2000).
- [7] K. G. Lagoudakis, M. Wouters, M. Richard, A. Baas, I. Carusotto, R. Andre, L. E. S. I. Dang, and B. Deveaud-Pledran, Quantized vortices in an exciton-polariton condensate, *Nature Physics* **4**, 706 (2008).
- [8] C. A. Jones and P. H. Roberts, Motions in a Bose condensate. IV. Axisymmetric solitary waves, *Journal of Physics A: Mathematical and General* **15**, 2599 (1982).
- [9] N. Meyer, H. Proud, M. Perea-Ortiz, C. O'Neale, M. Baumert, M. Holyński, J. Kronjäger, G. Barontini, and K. Bongs, Observation of Two-Dimensional Localized Jones-Roberts Solitons in Bose-Einstein Condensates, *Physical Review Letters* **119**, 150403 (2017).
- [10] N. N. Bogoliubov, On the Theory of Superfluidity, *Journal of Physics (USSR)* **11**, 23 (1947).
- [11] L. Onsager, Statistical hydrodynamics, *Il Nuovo Cimento (1943-1954)* **6**, 279 (1949).
- [12] G. Gauthier, M. T. Reeves, X. Yu, A. S. Bradley, M. A. Baker, T. A. Bell, H. Rubinsztein-Dunlop, M. J. Davis, and T. W. Neely, Giant vortex clusters in a two-dimensional quantum fluid, *Science* **364**, 1264 (2019).
- [13] S. P. Johnstone, A. J. Groszek, P. T. Starkey, C. J. Billington, T. P. Simula, and K. Helmerson, Evolution of large-scale flow from turbulence in a two-dimensional superfluid, *Science* **364**, 1267 (2019).
- [14] Y. Kawaguchi and M. Ueda, Spinor Bose-Einstein condensates, *Physics Reports* **520**, 253 (2012).
- [15] Y. J. Lin, K. Jimenez-Garcia, and I. B. Spielman, Spin-orbit-coupled Bose-Einstein condensates, *Nature* **470**, 83 (2011).
- [16] T. Bland, G. Lamporesi, M. J. Mark, and F. Ferlaino, Vortices in dipolar Bose-Einstein condensates, *Comptes Rendus. Physique* **24**, 133 (2023).
- [17] C. Ticknor, R. M. Wilson, and J. L. Bohn, Anisotropic Superfluidity in a Dipolar Bose Gas, *Physical Review Letters* **106**, 065301 (2011).
- [18] B. C. Mulkerin, R. M. W. van Bijnen, D. H. J. O'Dell, A. M. Martin, and N. G. Parker, Anisotropic and Long-Range Vortex Interactions in Two-Dimensional Dipolar Bose Gases, *Physical Review Letters* **111**, 170402 (2013).
- [19] E. Casotti, E. Poli, L. Klaus, A. Litvinov, C. Ulm, C. Politi, M. J. Mark, T. Bland, and F. Ferlaino, Observation of vortices in a dipolar supersolid, *Nature* **635**, 327 (2024).
- [20] M. R. Andrews, C. G. Townsend, H. J. Miesner, D. S. Durfee, D. M. Kurn, and W. Ketterle, Observation of interference between two Bose condensates, *Science* **275**, 637 (1997).
- [21] J. Stenger, S. Inouye, A. P. Chikkatur, D. M. Stamper-Kurn, D. E. Pritchard, and W. Ketterle, Bragg Spectroscopy of a Bose-Einstein Condensate, *Physical Review Letters* **82**, 4569 (1999).
- [22] S. W. Seo, B. Ko, J. H. Kim, and Y. Shin, Observation of vortex-antivortex pairing in decaying 2D turbulence of a superfluid gas, *Scientific Reports* **7**, 4587 (2017).
- [23] C. Nore, M. Abid, and M. E. Brachet, Kolmogorov Turbulence in Low-Temperature Superflows, *Physical Review Letters* **78**, 3896 (1997).
- [24] A. S. Bradley and B. P. Anderson, Energy Spectra of Vortex Distributions in Two-Dimensional Quantum Turbulence, *Physical Review X* **2**, 041001 (2012).
- [25] A. S. Bradley, R. K. Kumar, S. Pal, and X. Yu, Spectral analysis for compressible quantum fluids, *Physical Review A* **106**, 043322 (2022).
- [26] Q. Glorieux, T. Aladjidi, P. D. Lett, and R. Kaiser, Hot atomic vapors for nonlinear and quantum optics, *New Journal of Physics* **25**, 051201 (2023).
- [27] M. Abobaker, W. Liu, T. Aladjidi, A. Bramati, and Q. Glorieux, Inverse energy cascade in two-dimensional quantum turbulence in a fluid of light (2022), arXiv:2211.08441 [cond-mat, physics:quant-ph].
- [28] M. Naraschewski and R. J. Glauber, Spatial coherence and density correlations of trapped Bose gases, *Physical Review A* **59**, 4595 (1999).
- [29] T. Z. Fischer and A. S. Bradley, Regimes of steady-state turbulence in a quantum fluid, *Physical Review A* **111**, 023308 (2025).
- [30] A. Kolmogorov, The Local Structure of Turbulence in Incompressible Viscous Fluid for Very Large Reynolds' Numbers, *Akademiia Nauk SSSR Doklady* **30**, 301 (1941).
- [31] E. A. Novikov, Dynamics and statistics of a system of vortices, *Zhurnal Eksperimental'noi i Teoreticheskoi Fiziki* **68**, 1868 (1975).
- [32] A. Skaugen and L. Angheluta, Origin of the inverse energy cascade in two-dimensional quantum turbulence, *Physical Review E* **95**, 1868 (2017).
- [33] M. Baker-Rasooli, T. Aladjidi, N. A. Krause, A. S. Bradley, and Q. Glorieux, Observation of Jones-Roberts solitons in a paraxial quantum fluid of light (2025), arXiv:2501.08383 [cond-mat].
- [34] T. W. Neely, A. S. Bradley, E. C. Samson, S. J. Rooney, E. M. Wright, K. J. H. Law, R. Carretero-González, P. G. Kevrekidis, M. J. Davis, and B. P. Anderson, Characteristics of Two-Dimensional Quantum Turbulence in a Compressible Superfluid, *Physical Review Letters* **111**, 235301 (2013).
- [35] N. Navon, A. L. Gaunt, R. P. Smith, and Z. Hadzibabic, Emergence of a turbulent cascade in a quantum gas, *Nature* **539**, 72 (2016).
- [36] A. L. Fetter and A. A. Svidzinsky, Vortices in a trapped dilute Bose-Einstein condensate, *Journal of Physics: Condensed Matter* **13**, R135 (2001).
- [37] Z. Mehdi, J. J. Hope, S. S. Szigeti, and A. S. Bradley, Mutual friction and diffusion of two-dimensional quantum vortices, *Physical Review Research* **5**, 013184 (2023).
- [38] N. A. Krause and A. S. Bradley, Thermal decay of planar Jones-Roberts solitons, *Physical Review A* **110**, 053302 (2024).
- [39] S. Tsuchiya, F. Dalfó, and L. Pitaevskii, Solitons in two-dimensional Bose-Einstein condensates, *Physical Review A* **77**, 10.1103/physrev.77.045601 (2008).
- [40] A. Fetter and J. k Kim, Vortex precession in a rotating nonaxisymmetric trapped Bose-Einstein condensate, *Journal Of Low*

- Temperature Physics **125**, 239 (2001).
- [41] C. A. Jones, S. J. Putterman, and P. H. Roberts, Motions in a Bose condensate. V. Stability of solitary wave solutions of non-linear Schrodinger equations in two and three dimensions, *Journal Of Physics A-Mathematical And General* **19**, 2991 (1986).
- [42] O. Fialko, A. S. Bradley, and J. Brand, Quantum Tunneling of a Vortex between Two Pinning Potentials, *Physical Review Letters* **108**, 015301 (2012).
- [43] There is a lower bound due to the requirement that the density remain positive.
- [44] This is nothing more than an application of the Wiener-Khinchin theorem under angular integration.
- [45] The local velocity correlation is finite outside the dipole separation scale, but vanishes under angular averaging.
- [46] Our calculation is equivalent to retaining only the leading term in an expansion in powers of $v^2/c^2 < 1$. Including higher orders can in principle be done (next order also captures the second much weaker peak in the spectrum, however the correlation function is no longer accessible analytically). Here we are only interested in the dominant length scale in the two-point correlator, captured by the leading term.
- [47] M. T. Reeves, T. P. Billam, B. P. Anderson, and A. S. Bradley, Inverse Energy Cascade in Forced Two-Dimensional Quantum Turbulence, *Physical Review Letters* **110**, 104501 (2013).
- [48] M. T. Reeves, T. P. Billam, B. P. Anderson, and A. S. Bradley, Identifying a Superfluid Reynolds Number via Dynamical Similarity, *Physical Review Letters* **114**, 155302 (2015).